

Size of the Light-Emitting Region in a Sonoluminescing Bubble

Jeppe Seidelin Dam and Mogens T. Levinsen*

Biocomplexity Lab, Niels Bohr Institute, Blegdamsvej 17, DK-2100 Copenhagen Ø, Denmark
(Received 26 May 2003; revised manuscript received 29 December 2003; published 8 April 2004)

The size of the light-emitting region is a key parameter toward understanding the light-emitting processes in a sonoluminescing bubble. Here we present measurements of interference effects from particles with a diameter of approximately $2\ \mu\text{m}$ situated $6\text{--}10\ \mu\text{m}$ from a sonoluminescing bubble. From the angular size of the pattern and from an estimated distance to the particles we conclude that the light-emitting region of a sonoluminescing bubble is smaller than commonly believed {see, e.g., S. Hilgenfeldt, S. Grossman, and D. Lohse [Nature (London) **398**, 402 (1999)]}. We argue that an upper limit of the size of the light-emitting region is approximately 200 nm.

DOI: 10.1103/PhysRevLett.92.144301

PACS numbers: 78.60.Mq, 47.52.+j, 47.55.Bx

Knowledge of the size of the light-emitting region is of key interest in the understanding of light-emitting processes in a sonoluminescing bubble. However, different theories predict not only different temperatures and degree of opacity, but also much different sizes of the light-emitting region. Some models (see, e.g., the key paper by Hilgenfeldt *et al.* [1]) view conditions inside the bubble as uniform, whereas others suggest considerable differences in pressures, and thus temperatures, throughout the bubble [2–4] leading to a smaller and hotter light-emitting region.

Here we present some exciting new experimental results that offer a surprising way of measuring this elusive quantity.

Trentalange and Pandey [5] proposed using Hanbury Brown–Twiss (HBT) single photon correlation to measure the size of the light-emitting region. In Ref. [6] it is found that doing this requires an immense amount of data (correlating of the order of 10^{10} pulses from several channels) especially since, as will be seen, individual time tracks have to be recorded. To the authors' knowledge no results from such measurements have yet been published. In fact, our experiment was originally designed for making the HBT measurement, but so far we have not reached any conclusions. However, in the process of analyzing our data, we found [7–9] (see Figs. 1 and 2 in Ref. [7]) that the autocorrelations are higher than the cross correlations. This experimental fact raised questions, to which we now believe we not only have the answers, but also that from these we can draw conclusions regarding the size of the light-emitting region.

The experimental setup is described in detail in Ref. [8]. We use three optical fibers (1 mm) 6 cm from the center of a spherical cell (diameter 6 cm corresponding to a resonance of ~ 25.1 kHz). The optical fibers are mounted near each other as shown in Fig. 1. The angles between fibers as seen from the bubble are calculated using the distances between the centers of the fiber openings and the distance to the center of the flask. The fibers connect to photomultiplier tubes (PMT), which are connected to separate

amplifying systems. A computer registers the maximum amplitude of the flashes. As the fibers are relatively thin, covering only a solid angle of 0.4 msrad, and thus catch only a few photons per flash, we usually make a running average of the amplitude of 20 flashes to clearly discern any interesting features.

Visual inspection of the averaged time tracks revealed the presence of some prominent features. In one fiber (channel), e.g., the light intensity suddenly drops to about 50%, rises to over 200%, and then drops down to 50% again. With some overlap, this is seen in another channel. This happens in a time span of 400 flashes (16 ms). The highest relative intensity fluctuations we have observed are down to 30% and up to 500% while the duration in time varies from 25 to 1000 flashes. Often secondary peaks are also seen. The structures are never being seen simultaneously in fibers placed 15° or more apart (including fibers 180° apart). This rules out the effect being directly coupled to the bubble dynamics. The phenomenon is observed at all drive pressures and argon contents, for which stable sonoluminescence with reasonable intensity can be obtained.

These features are responsible for the initial enhancement of the autocorrelations seen in Fig. 1 of Ref. [7].

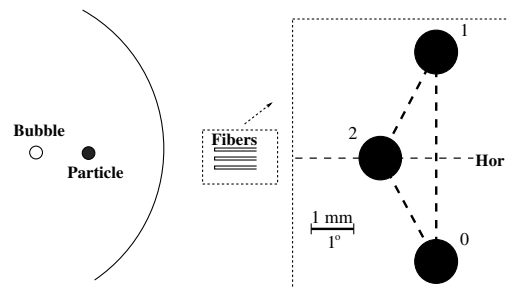


FIG. 1. Configuration of the experiment. In the enlargement the fibers are seen end on from the bubble, “Hor” being the horizontal plane. The angular distance, as seen from the bubble, between fibers 0 and 2 and 1 and 2 is 2.75° , while the distance between 0 and 1 is 4.76° . The solid angle viewed by fiber is 0.4 msrad.

However, since they only are seen nearly simultaneously with fibers placed close together, they will not affect cross correlations for fibers placed far apart as when studying the spatial dependence of period doubling. As regards the Hanbury Brown–Twiss effect though, the features introduce a disastrous bias.

Quite a few possibilities come to mind when trying to deduce the origin of the features. The sheer size, the secondary peaks, and the fact that they are not seen when a larger solid angle (50 msrad) is employed all suggest that the features can be explained by an interference pattern with a central peak slowly traversing the fibers. The most likely way for such a pattern to be produced is a dust particle being strobed by the bubble while passing the line of sight to the fiber. Such particles are known to be attracted to the bubble after some time (see Fig. 2 in Weninger *et al.* [10] and also Ref. [11]). Partly because interference thus seems the most plausible cause, but also because of the extremely interesting conclusions that may be drawn regarding the size and nature of the emitting region inside the bubble, we concentrate on this explanation. Later we discuss other possible scenarios and why these can be refuted.

In order to check the hypothesis of interference caused by a nearby small particle we cleaned the system carefully and refilled with water passed through two consecutive 0.2 μm millipore filters. Repeating the measurement twice with water cleaned in this fashion showed the features to be extremely rare, if at all present (a few per hour). We then added to the water a drop containing poly(methyl methacrylate) (PMMA) particles of size $6 \pm 1.8 \mu\text{m}$ having a refractive index of 1.49 resulting in 5 ppm solid mass (manufacturer Polysciences Inc.). The size and refractive index are chosen to match those of common dust [12].

Immediately the patterns reappeared, leaving little doubt about the validity of our interpretation. An example is shown in Fig. 2(a). However, now we not only see features like those already described above, but also less prominent, larger angle features [as estimated from their

overlap of all three fibers; see Fig. 2(b)], consistent with interference patterns originating from larger particles or even simple shadowing by large particles. With the large spread in particle size, this is to be expected.

From Figs. 1 and 2(a) it can be deduced that the size of the interference pattern measured from maximum to minimum intensity for this particular case is about 5° , i.e., the distance between the most distant detectors. (Notice that structures less than of order 1° would be smeared across the opening of the fiber.) A noteworthy difference is that the patterns with a strong middle peak are always of size 5° for the PMMA particle while always of size 3° for the dust particles. This is a consequence of the stringent requirements set by the condition of strong constructive interference. We should add that we have tried polystyrene particles of sizes 0.40, 1.05, and 2.84 μm of narrow distributions. These have a refractive index of 1.58 and are not seen.

If the interference patterns are a result of diffraction by a nearby particle presumably having a higher index of refraction than water, simultaneous measurements of the distance between particle and bubble can be used to calculate an upper limit on the size of the light-emitting region. To this end, notice that if the angular size of the light-emitting region, as seen from the particle, is larger than 5° , the interference effect would be quenched. Light emitted from the center of the bubble will result in an interference peak directly behind the particle. Light emitted from a point some distance away from the center will also result in a peak; however, this peak would be displaced, being directly behind the particle as seen from the point of light emission. Thus, to produce the observed peaks, the light-emitting region, as seen from the particle, has to be significantly smaller than the angular size of the observed interference pattern. The validity of this postulate has been checked by superposition of suitably chosen interference patterns. As the interference pattern is of a size near 5° , the light-emitting region must be smaller than 5° , observed from the particle. If we assume that the particle is placed 10 μm from the bubble, in accordance with Weninger *et al.* [10], an upper limit of the size of the light-emitting region can be estimated.

$$s \ll \sin(5^\circ) \times 10 \mu\text{m} = 0.9 \mu\text{m}. \quad (1)$$

Thus the radius s of the light-emitting region would have an upper limit of a few hundred nanometers, i.e., significantly less than the minimum radius of the bubble. In effect the upper limit of the light-emitting region is determined by only two factors, namely, the angular size of the resulting interference pattern and the distance between the light-emitting region and the particle at the time of light emission. Calculations on the following model of interference effects from a particle confirm these results suggesting a distance to this of approximately 6 μm giving $s \ll 0.5 \mu\text{m}$.

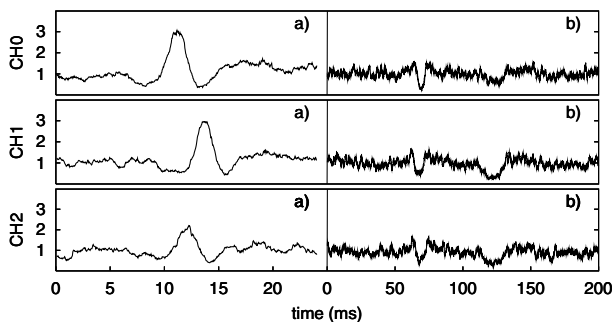


FIG. 2. Interference patterns caused by PMMA particles. Notice that the patterns in (a) are not exactly simultaneous in the three channels while in (b) there is a nearly complete overlap. Running average over 30 flashes (~ 1.2 ms).

The model is constructed as follows. The light source is modeled as a isotropic point source emitter in water at a given distance from the particle. The amplitude observed at large distances is now calculated according to an integral of Kirchhoff's equation [13] over a spherical shell centered on the source and containing the particle (see Fig. 3). The wave amplitude is in the model assumed to be constant over the entire shell. The phase of the wave is also constant upon the shell—except for the small region occupied by the particle, where the lower velocity of light in the particle shifts the phase. However, reflection, etc., inside the particle is neglected. The change θ in relative phase can be estimated as

$$\theta = \frac{2\pi d(1.49 - 1.33)}{\lambda}. \quad (2)$$

Here d is the distance traveled through the particle and λ is the wavelength. The refractive index of water is 1.33 compared to that of the particle of 1.49. To obtain a significant interference effect from such a particle, the phase change must be at least of order π . With the spectral response of our detection system in mind (maximum near 300 nm, see Fig. 2 in Ref. [8]), this translates to particles with a diameter of order $1 \mu\text{m}$, a common size for dust particles according to [12]. Calculations on the model, as well as on the model discussed in the next paragraph, suggest that the distance between bubble and particle is $5\text{--}10 \mu\text{m}$ which is in good agreement with Fig. 2A in Ref. [10]. An example of a pattern calculated using the model is shown in Fig. 3 revealing a close resemblance to the observed patterns.

The minimum possible distance between particle and the center of the bubble at the point of light emission can be estimated using the following argument. The amount of water closer to the bubble wall than the center of the particle remains constant over one full acoustic cycle, as the particle moves along with the water. A lower limit is given by the center of the particle not being able to get closer than one particle radius at the point of maximum bubble radius. This minimal amount of water between bubble and particle corresponds to a distance of around

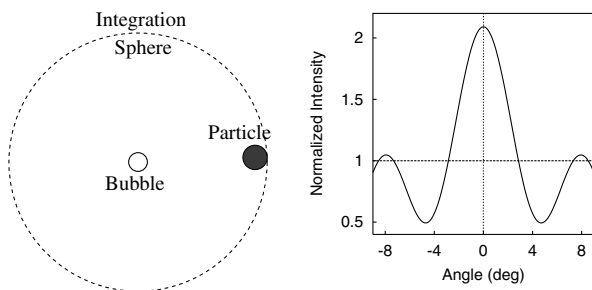


FIG. 3. The model used for the calculation of the interference pattern created by a particle close to the bubble. The pattern calculated from the model using particle diameter $2 \mu\text{m}$, distance $6 \mu\text{m}$, and refractive index 1.49.

$10 \mu\text{m}$ at the point of light emission, depending on the radius of the particle and the bubble parameters.

In some cases we observe a peculiar phenomenon (here for a dust particle). An example is shown in Fig. 4. These patterns are seen to occur repeatedly every 2150 flashes more or less clearly for more than 150 times. Sometimes the interference patterns occur in a manner suggestive of the strobed position of a particle passing by with different directions for each occurrence. The repetition of the strobed positions of the particle is not inconsistent with the simulations of streamlines by Verraes *et al.* [14] as shown in their Fig. A1 with the particle being dragged along by the velocity field. Similar short series of periodic behavior, although never as clear as in the case described above, have periodicity ranging from 900–20 000 flashes. A recent measurement [15] with vesicles caught in the flow near a bubble oscillating on a solid surface shows these moving in the flow field and reappearing with a constant frequency similar to our observations in Fig. 4.

Of course other explanations can be imagined. Turning the argument of Eq. (1) upside down, if the light-emitting region covers the whole interior of the bubble more or less uniformly then the distance to a particle should be $\gg 20 \mu\text{m}$. However, a distant particle would have to be large thus acting as a classical spherical lens. With a refractive index of 1.5 the particle should, however, cover an angle of 15° seen from the bubble in order to reach the central peak height observed, but this is now narrow and surrounded by a large dark region while no secondary peaks are possible. Regarding the regular recurrence of the pattern, it seems more likely that a particle close to the bubble is caught in some kind of a vertex and thus reappears every so often, than would a distant particle. The observed patterns could also result from other phenomena; e.g., if an ingoing jet is formed, the resulting shape of the bubble could be the focusing mechanism. A drift in the position of the jet then explains the change of direction of the features. For other reasons, however, jets are not likely to occur in sonoluminescence far from boundaries (see, e.g., Ref. [16]). Furthermore, it is unlikely that the occurrence of a jet should not have consequences for the emission in other directions.

These alternative explanations have severe problems with reproducing the shape of the patterns even if they are able to produce the magnitude and angular size of this. From this and the reasons stated above, we conclude that the patterns do originate in close-by particles.

To summarize our present Letter, in a previous Letter [7] we presented a correlation analysis. We show here that the elevated autocorrelations (with respect to the cross correlations) are due to the presence of nearby dust particles giving rise to interference. The particles have no effect on the cross correlation from the larger angles, as the size of the interference pattern is small.

Further measurements are needed to pin down the exact size of the light-emitting region. This could be

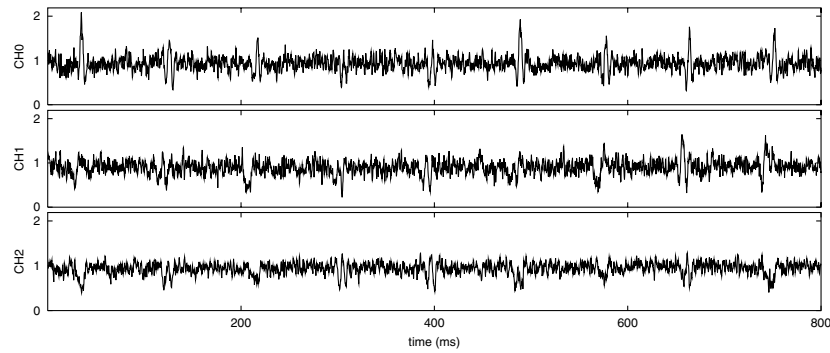


FIG. 4. Interference patterns occur with a fixed frequency. Running average over 20 flashes (~ 0.8 ms).

done with small angle detectors fitted with short-pass (500 nm) filters viewing from one direction. At an angle of 90° a camera mounted on a long distance microscope is placed using a longer wavelength, pulsed light source to illuminate the bubble and potential particle. Thus one could simultaneously measure the size of the interference pattern and the particle to bubble distance, i.e., the two essential parameters when calculating the upper limit of the size of the light-emitting region. To further improve the experiment, spherical particles with a narrow size distribution should be used. Intimate knowledge regarding the particles would in all circumstances make for a better model—and quite possibly allow one to estimate the actual size, shape, and opacity of the light-emitting region. Furthermore, valuable information regarding the flow around the bubble may be extracted from the regular recurrence of the particles and the apparent shifting directions of passage. These observations could also give a clue to the distance between bubble and particle.

Our interpretation of the features as interference patterns coupled with our model calculations suggest that the radius of the light-emitting region is much less than $0.5 \mu\text{m}$. This is in agreement with model calculations by Moss *et al.* [2,17] and Burnett *et al.* [18], who find that the light emission is from an optically thick core ($\sim 0.1 \mu\text{m}$) with an optically thin halo surrounding it.

The validity of this picture is supported by recent measurements of anisotropic light emission and period doubling [7–9]. An important probable consequence is that the temperature in the center is much higher than the approximately 15 000 K given by the uniform model [1].

The authors acknowledge financial support from the Danish National Science Foundation. We thank Martin Skogstad for help with the experiment and valuable discussions.

*Electronic address: levinsen@nbi.dk

- [1] S. Hilgenfeldt, S. Grossman, and D. Lohse, *Nature* (London) **398**, 402 (1999).
- [2] William C. Moss, Douglas B. Clarke, and David A. Young, *Science* **276**, 1398 (1997).
- [3] S. Putterman *et al.* *Nature* (London) **409**, 782 (2001).
- [4] Steven J. Ruuth, Seth Putterman, and Barry Merriman, *Phys. Rev. E* **66**, 036310 (2002).
- [5] S. Trentalange and S. U. Pandey, *J. Acoust. Soc. Am.* **99**, 2439 (1996).
- [6] C. Slotta and U. Heinz, *Phys. Rev. E* **58**, 526 (1998).
- [7] J. S. Dam, M. T. Levinsen, and M. Skogstad, *Phys. Rev. Lett.* **89**, 084303 (2002).
- [8] Jeppe Seidelin Dam, Mogens T. Levinsen, and Martin Skogstad, *Phys. Rev. E* **67**, 026303 (2003).
- [9] Mogens T. Levinsen, Nick Weppenaar, Jeppe Seidelin Dam, Gabor Simon, and Martin Skogstad, *Phys. Rev. E* **68**, 035303 (2003).
- [10] K. Weninger, P. G. Evans, and S. J. Putterman, *Phys. Rev. E* **61**, R1020 (2000).
- [11] S. Hyashi, S. Uchiyama, and N. Harba, *J. Phys. Soc. Jpn.* **70**, 3544 (2001).
- [12] Patrick Chazette and Catherine Liousse, *Atmos. Environ.* **35**, 2497 (2001).
- [13] R. W. Ditchburn, *Light* (Academic Press, London, 1976).
- [14] T. Verraes, F. Lepoint-Mullie, and T. Lepoint, *J. Acoust. Soc. Am.* **108**, 117 (2000).
- [15] P. Marmottant and S. Hilgenfeldt, *Nature* (London) **423**, 153 (2003).
- [16] M. P. Brenner, S. Hilgenfeldt, and D. Lohse, *Rev. Mod. Phys.* **74**, 425 (2002).
- [17] William C. Moss, David A. Young, Judith A. Harte, Joanne L. Levatin, Balazs F. Rozsnyai, George B. Zimmerman, and I. Harold Zimmerman, *Phys. Rev. E* **59**, 2986 (1999).
- [18] P. D. S. Burnett, D. M. Chambers, D. Heading, A. Machacek, M. Schnittker, W. C. Moss, P. Young, S. Rose, R. W. Lee and J. S. Wark, *J. Phys. B* **34**, L511 (2001).